

Cog2Gen3D: Sculpturing 3D Semantic-Geometric Cognition for 3D Generation

Haonan Wang¹, Hanyu Zhou^{2*}, Haoyue Liu¹, Tao Gu³, and Luxin Yan¹

¹ School of Artificial and Automation, Huazhong University of Science and Technology

² School of Computing, National University of Singapore

³ School of Computing, Macquarie University

whn_aurora@hust.edu.cn, hy.zhou@nus.edu.sg

Abstract. Generative models have achieved success in producing semantically plausible 2D images, but it remains challenging in 3D generation due to the absence of spatial geometry constraints. Typically, existing methods utilize geometric features as conditions to enhance spatial awareness. However, these methods can only model relative relationships and are prone to scale inconsistency of absolute geometry. Thus, we argue that semantic information and absolute geometry empower 3D cognition, thereby enabling controllable 3D generation for the physical world. In this work, we propose Cog2Gen3D, a 3D cognition-guided diffusion framework for 3D generation. Our model is guided by three key designs: 1) **Cognitive Feature Embeddings.** We encode different modalities into semantic and geometric representations and further extract logical representations. 2) **3D Latent Cognition Graph.** We structure different representations into dual-stream semantic-geometric graphs and fuse them via common-based cross-attention to obtain a 3D cognition graph. 3) **Cognition-Guided Latent Diffusion.** We leverage the fused 3D cognition graph as the condition to guide the latent diffusion process for 3D Gaussian generation. Under this unified framework, the 3D cognition graph ensures the physical plausibility and structural rationality of 3D generation. Moreover, we construct a validation subset based on the Marble World Labs. Extensive experiments demonstrate that our Cog2Gen3D significantly outperforms existing methods in both semantic fidelity and geometric plausibility.

Keywords: 3D Generation · 3D Cognition · Latent Diffusion Models

1 Introduction

Generative models have achieved success in synthesizing semantically plausible 2D images, which are widely used in image editing [1] and video generation [2]. When applying these models to the physical world, some researchers rely on the semantic priors of 2D diffusion models and extend them to 3D generation through Score Distillation Sampling [3,4], as illustrated in Fig. 1 (a). However, this

* Corresponding author.

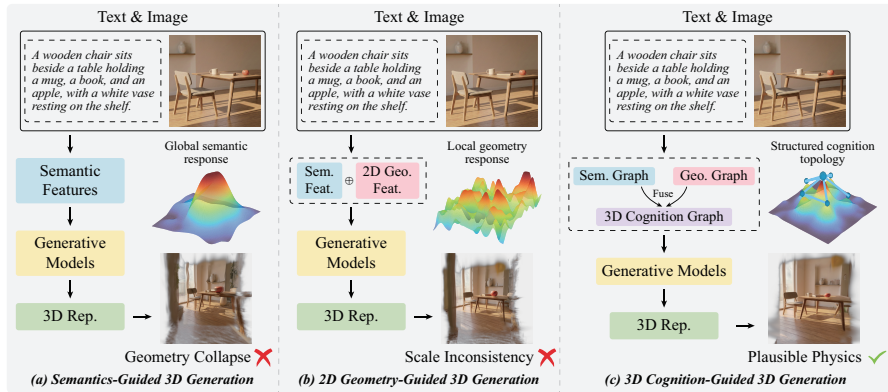


Fig. 1: Paradigm shift of 3D generation. Semantic-Guided Generation relies heavily on 2D semantic priors, resulting in physical violations such as object intersections. 2D Geometry-Guided 3D Generation introduces relative geometric constraints but frequently suffers from scale inconsistency due to the lack of absolute metric awareness. Our 3D Cognition-Guided paradigm leverages a 3D cognition graph as the condition, ensuring 3D generation with fidelity and plausibility.

paradigm is prone to structural collapse due to the lack of geometric constraints required by the physical world. In this work, our purpose is to integrate geometric and semantic representations to jointly achieve high-quality 3D generation.

As shown in Fig. 1 (b), existing methods mainly incorporate geometric priors such as scene graphs [5–9] and layouts [10–14] to enhance spatial awareness in the 3D generation process. For example, EchoScene [9] utilizes scene graphs to define relational dependencies between objects, while Layout2Scene [14] relies on bounding box layouts to guide the coarse spatial arrangement of the scene. However, these approaches are limited to modeling 2D relative spatial relationships and fail to capture 3D absolute geometry. This leads to scale inconsistency and geometric collapse, making it difficult to satisfy the rigid constraints of the physical world. Therefore, we argue that the key to 3D generation for the physical world lies in the integration of high-level semantics and absolute geometry.

To address the above issues, we propose that high-level semantics and 3D absolute geometry jointly empower 3D cognition and enhance the physical spatial awareness of 3D generation, as illustrated in Fig. 1 (c). Our design is grounded in two key insights: 1) Geometric features provide *essential physical plausibility*. We figure out that geometric encoders inherently capture dense correspondence and absolute metric information, which motivates us to leverage these cues to enforce strict physical constraints and precise scale consistency within the generative process. 2) Latent scene graphs provide *structural rationality* and *superior reasoning robustness*. We discover that latent scene graphs robustly infer topological relationships in a latent embedding space, which inspires the design of our graph module to ensure the coherent structure of the generated scenes. Thus, these observations motivate us to design a common-based fusion scheme that integrates semantic knowledge and geometric information to represent 3D cognition, thereby enabling controllable 3D generation for the physical world.

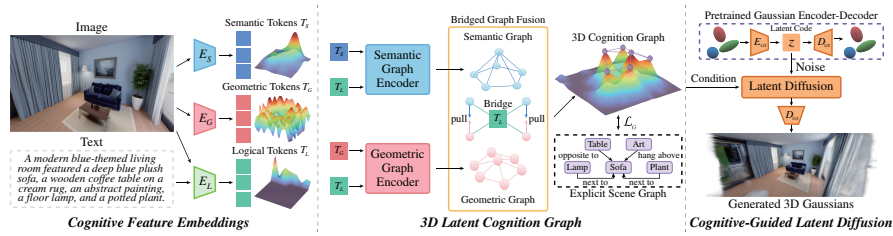


Fig. 2: Overview of Cog2Gen3D. The model first extracts multiple cognitive tokens (T_S, T_G, T_L). These tokens are structured into a 3D Cognition Graph, where the logical tokens act as a bridge for semantic-geometric alignment. Finally, the awakened 3D cognition steers a latent diffusion process to generate 3D Gaussians.

In this work, we propose **Cog2Gen3D**, a novel 3D cognition-guided diffusion framework for 3D generation. Our model consists of three key components: 1) **Cognitive Feature Embeddings**. We encode different input modalities into semantic and geometric representations and further extract logical representation to serve as high-level guidance. 2) **3D Latent Cognition Graph**. We structure these representations into dual-stream semantic-geometric graphs and utilize the logical representation as a bridge to fuse them via common-based cross-attention, obtaining a unified 3D cognition graph. 3) **Cognition-Guided Latent Diffusion**. We leverage the 3D cognition graph as condition to guide the diffusion process for 3D Gaussian generation. Through this design, our approach effectively awakens 3D cognition, ensuring that the generated scenes possess both high-fidelity semantics and plausible geometry. Our main contributions are summarized as follows:

- We propose **Cog2Gen3D**, an innovative framework that introduces 3D cognition to guide 3D generation, effectively bridging semantic priors with geometric constraints to support versatile controllable 3D object and scene generation from arbitrary combinations of visual and textual prompts.
- We observe that geometric features provide geometry consistency and latent scene graphs offer structural rationality. This motivates the design of cognitive feature embeddings and 3D latent cognition graph for sculpturing a robust 3D representation that captures appearance attributes and spatial interactions.
- We develop a cognition-guided latent diffusion mechanism that steers 3D Gaussian generation using the cognition graph, ensuring both semantic fidelity and geometric plausibility of the generated 3D scenes.
- We integrate a series of 3D datasets and construct a curated validation subset, collectively named the cognition scene graph 3D dataset (**CogSG-3D**), along with explicit scene graph labels for supervision. Extensive experiments have demonstrated the significant effectiveness of our method.

2 Related Works

2.1 Semantics-Guided 3D Generation

The success of 2D diffusion models has significantly advanced 3D generation. Current methods predominantly leverage their rich semantic priors to supervise

3D representations [3,4,15–18]. For instance, DreamFusion [3] lifts 2D image priors via Score Distillation Sampling (SDS) to iteratively optimize a 3D model. While capable of synthesizing visually impressive objects, these approaches struggle with severe geometric collapse. This limitation arises because they treat 3D generation as multi-view 2D in-painting, lacking an intrinsic perception of physical spatial structures. Therefore, our goal is to introduce geometric cues into the generative process to ensure both appearance fidelity and structural rationality.

2.2 2D Geometry-Guided 3D Generation

To mitigate structural inconsistencies, recent approaches explicitly incorporate 2D geometric priors, such as scene graphs [5–8] and layouts [10–13], to organize global scene composition. For instance, EchoScene [9] utilizes topological structures to constrain the semantic interactions among entities, whereas Layout2Scene [14] relies on bounding boxes to restrict the relative positions of generated objects. While these structured representations successfully provide a reasonable blueprint to produce roughly arranged scenes, they persistently struggle to ensure precise physical plausibility and strict structural fidelity in complex environments. This limitation fundamentally arises because these methods predominantly model 2D relative spatial relationships rather than the precise absolute metric geometry of the 3D physical world. Consequently, our work focuses on capturing 3D absolute geometry to sculpt structurally rigorous and physically plausible 3D scenes.

2.3 Spatial Geometric Perception

Spatial geometric perception is crucial for 3D generation, as it bridges image-text prompts and structurally rigorous 3D scenes. The core of this perception lies in accurately capturing absolute metric geometry rather than merely coarse topological relations. Recent spatial representation models, such as VGGT [19], have demonstrated exceptional capabilities in encoding fine-grained 3D spatial geometry. However, effectively integrating such perception into generative models remains a challenge. Existing Multimodal Large Language Models often resort to naive feature concatenation [20,21], which fails to deeply assimilate precise geometric constraints. In contrast, we propose to construct a structured geometric graph and fuse it with a corresponding semantic graph. This design effectively awakens 3D cognition, ensuring both the physical plausibility and structural rationality of the synthesized 3D scenes.

3 Our Cog2Gen3D

Overview. As shown in Fig. 2, our Cog2Gen3D achieves semantically-coherent and geometrically-plausible 3D generation through the following three stages:

1) **Cognitive Feature Embeddings.** This is the cognitive representation stage that we transform input images I and texts T into disentangled semantic, geometric, and logical representations T_S, T_G, T_L :

$$T_S, T_G, T_L = E_{S,G,L}(I, T), \quad (1)$$

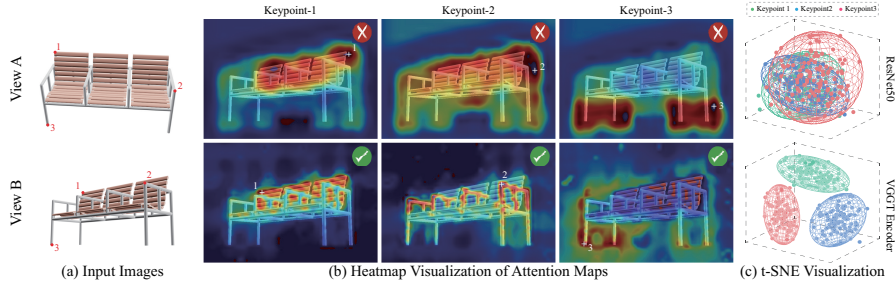


Fig. 3: Cross-view feature correspondence analysis. The attention map and the t-SNE visualization demonstrate that the VGGT encoder has superior cross-view geometric consistency. This validates its capability of capturing absolute geometry information, which motivates us to introduce VGGT encoder as our geometric expert.

which serve as the fundamental building blocks for subsequent cognitive reasoning. 2) **3D Latent Cognition Graph.** This is the 3D cognition construction stage that we encode the extracted features into dual-stream graphs G_{sem} , G_{geo} and fuse them via a common-based fusion with the logical bridge T_L :

$$G_{sem} = GE(T_S, T_L), G_{geo} = GE(T_G, T_L), G_{cog} = ComFusion(G_{sem}, G_{geo}, T_L). \quad (2)$$

The resulting 3D cognition graph G_{cog} precisely captures both the extrinsic semantics and intrinsic geometry of the scene.

3) **Cognition-Guided Latent Diffusion.** This is the cognition-guided generation stage that the 3D cognition graph acts as a structural condition to steer the latent diffusion process, ultimately generating 3D Gaussians $\hat{\mathcal{G}}$ with high-fidelity appearance and rational structure:

$$\hat{\mathbf{z}}_0 = \text{LDM}(\mathbf{z}_T | G_{cog}), \hat{\mathcal{G}} = D_{GS}(\hat{\mathbf{z}}_0). \quad (3)$$

Remarks. The output $\hat{\mathcal{G}}$ denotes the generated 3D Gaussians representing the 3D scene with high-fidelity appearance and rational structure. Our framework utilizes a 3D latent cognition graph as structural conditions to enable semantically-coherent and geometrically-plausible 3D generation in diffusion models.

3.1 Cognitive Feature Embeddings

While conventional generative models rely predominantly on semantic priors, we establish a comprehensive foundation for 3D cognition by integrating semantic and geometric information alongside logical constraints.

Semantic Encoder (E_S). To capture rich visual appearance, we utilize a pre-trained ResNet50 [22] as the semantic encoder E_S . It extracts high-level visual features from input images and projects them into Semantic Tokens T_S , ensuring high-fidelity appearance in the generated 3D Gaussians.

Geometric Encoder (E_G). As illustrated in Fig. 3, we evaluate the feature representations of ResNet50 [22] and the VGGT encoder [19] by computing cross-view attention between the keypoint-specific features of View A and the spatial feature maps of View B. Visualizations reveal that ResNet50 struggles with feature drift while VGGT distinctly separates keypoint features, demonstrating robust

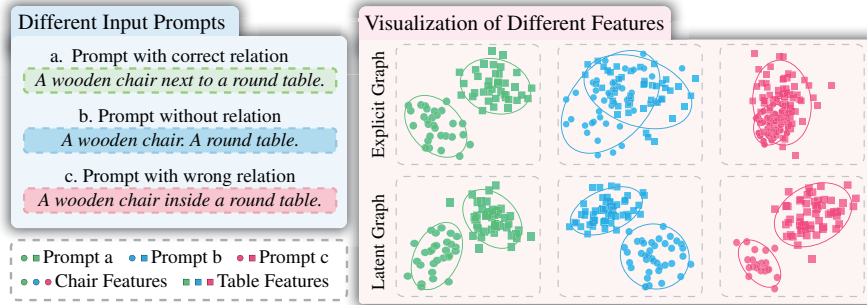


Fig. 4: Feature distribution of explicit vs. latent scene graphs under prompt perturbations. Explicit graphs diverge significantly when given missing or incorrect relations compared to the correct baseline. Conversely, our latent scene graph maintains a stable distribution, demonstrating superior robustness to unpromising prompts.

cross-view geometric consistency. Motivated by this capability, we adopt VGGT as our geometric encoder E_G , which provides essential geometric grounding, ensuring rigorous structural plausibility and metric accuracy.

Logical Encoder (E_L). To bridge raw features and structural reasoning, we adopt CLIP ViT and CLIP Text encoders [23] as the logical encoder E_L . By processing image-text pairs, E_L extracts Logical Tokens T_L that encapsulate high-level relational contexts and abstract concepts, serving as the essential guidance for constructing the 3D cognition of the scene.

Through this tri-stream architecture, we obtain a comprehensive set of cognitive tokens $\{T_S, T_G, T_L\}$, which collectively define the cognitive feature space required for the subsequent 3D Latent Cognition Graph construction.

3.2 3D Latent Cognition Graph

3D generation requires robust guidance equipped with both rich semantics and absolute geometry. Fig. 4 shows that explicit scene graphs are highly sensitive to noisy inputs, suffering from severe feature divergence under prompt perturbations. To address this, we propose the 3D Latent Cognition Graph. By processing cognitive tokens through a dual-stream latent graph encoder and a common-based fusion mechanism, this module implicitly sculpts a noise-resistant and structurally rigorous cognitive representation.

Dual-Stream Latent Graph Encoder. To capture coherent appearance and precise geometry, we construct two parallel graphs: a semantic graph and a geometric graph. Both share a similar topological encoding paradigm but differ fundamentally in their input tokens and positional embedding strategies.

Semantic Graph Construction. We formulate the semantic query Q_S by concatenating tokens T_S with a 2D positional embedding $PE(x_p, y_p)$. Through cross-attention between Q_S and T_S , we extract n initial nodes N_i^S ($i \in [0, n]$). To establish relationships, the cross-attention utilizes the shared logical tokens

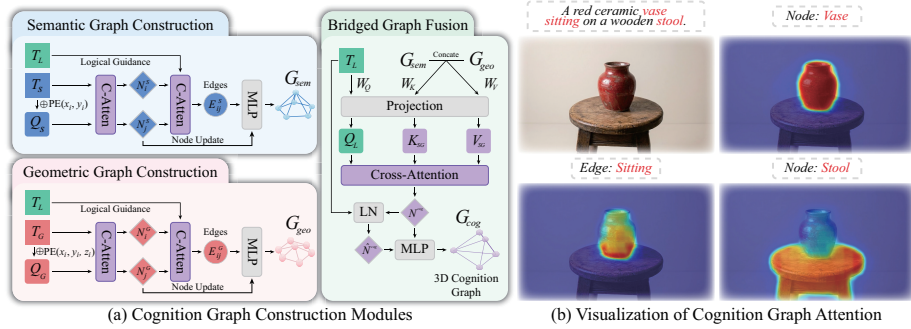


Fig. 5: Architectural details and interpretability of the 3D Latent Cognition Graph. (a) The pipeline for constructing cognition graph from cognitive tokens. (b) The correspondence visualization showing how graph components precisely align with 3D entities and spatial boundaries.

T_L as logical guidance to formulate semantic edges E_{ij}^S between N_i^S and N_j^S ($i, j \in [0, n]$). An MLP then utilizes the message m_{ij}^S from nodes and corresponding edges to update the nodes, thus obtaining the semantic graph G_{sem} :

$$m_{ij}^S = \text{MLP}(N_i^S, N_j^S, E_{ij}^S), \quad G_{sem} = N_i^S + \sum_j m_{ij}. \quad (4)$$

Geometric Graph Construction. To move beyond 2D constraints and model absolute 3D metrics, the geometric query Q_G employs a specialized 3D positional embedding $\text{PE}(x_q, y_q, z_q)$. Here, z_q is a learnable embedding explicitly introduced to capture underlying spatial geometry. Similar to the semantic stream, cross-attention modules extract initial nodes N_i^G and utilize T_L to formulate geometric edges E_{ij}^G . An MLP then updates them to produce the geometric graph G_{geo} . Driven by the learnable z_q dimension, this graph effectively models absolute 3D metric relationships between entities.

Common-based Cross-Attention Fusion. While the semantic and geometric graphs encapsulate coherent appearance and precise geometry respectively, they remain in separate feature spaces. Since both graphs utilize the same logical tokens T_L for relation edge E_{ij} formulation, their topologies inherently share a common logical foundation.

Exploiting this shared foundation, we introduce a common-based cross-attention fusion mechanism. To integrate the distinct feature spaces, we treat the logical tokens T_L as a unifying anchor. We project T_L to form a shared logical query Q_L , while the semantic and geometric nodes are concatenated along the feature dimension to jointly formulate the keys K_{sg} and values V_{sg} :

$$Q_L = T_L \mathbf{W}_Q, \quad \mathbf{K}_{SG} = [G_{sem} || G_{geo}] \mathbf{W}_K, \quad \mathbf{V}_{SG} = [G_{sem} || G_{geo}] \mathbf{W}_V, \quad (5)$$

where $[||\cdot]$ denotes the concatenation operation, and $\mathbf{W}_Q, \mathbf{W}_K, \mathbf{W}_V$ are learnable linear projection matrices. The unified 3D cognition graph nodes, denoted as \mathbf{N}^{cog} , are then computed via the scaled dot-product cross-attention:

$$\mathbf{N}^{cog} = \text{Softmax} \left(\frac{Q_L \mathbf{K}_{SG}^T}{\sqrt{d_k}} \right) \mathbf{V}_{SG}, \quad (6)$$

where d_k is the scaling factor representing the channel dimension. In this formulation, the logical query \mathbf{Q}_L acts as an intelligent bridge, adaptively assigning attention weights to extract and align corresponding semantic textures and structural constraints. Finally, we apply a residual connection and a MLP to stabilize the fused representation:

$$\hat{\mathbf{N}}^{cog} = \text{LayerNorm}(T_L + \mathbf{N}^{cog}), \quad \mathbf{G}_{cog} = \text{MLP}(\hat{\mathbf{N}}^{cog}) + \hat{\mathbf{N}}^{cog}. \quad (7)$$

Ultimately, this explicit mathematical fusion yields a holistic 3D cognition graph \mathbf{G}_{cog} that perfectly balances semantic coherence with geometric rationality, ready to structurally guide the subsequent 3D generative process.

3.3 Cognition-Guided Latent Diffusion

With the comprehensive 3D cognition graph formulated, the final stage of our framework is to effectively generate the 3D scenes with semantic fidelity and geometric plausibility. Therefore, we propose a cognition-guided latent diffusion process that operates within a compressed space of 3D Gaussians.

Conditioned Diffusion Process. Standard diffusion models acting directly on explicit 3D representations are often computationally prohibitive. Therefore, we perform the generative process in a learned latent space. Let the ground-truth latent representation of the 3D scene be denoted as \mathbf{z}_0 . During the forward diffusion process, Gaussian noise ϵ is progressively added to \mathbf{z}_0 over t timesteps, producing a noisy latent \mathbf{z}_t . In the reverse denoising process, our goal is to predict and remove this noise. Crucially, instead of relying on rudimentary text or layout conditions, we inject our fused cognition graph, \mathbf{G}_{cog} , as the structural condition. The denoising network predicts the added noise as:

$$\hat{\epsilon} = \epsilon_{\theta}(\mathbf{z}_t, t, \mathbf{G}_{cog}). \quad (8)$$

Within the denoising network, the high-fidelity semantics and plausible geometry embedded in \mathbf{G}_{cog} effectively guide the generation of the latent space. This cognition-guided paradigm effectively mitigates the geometric ambiguity and layout distortion commonly observed in standard 2D-prior-based generation.

Latent-Gaussian Encoder-Decoder. To bridge the gap between the compact latent space and the explicit 3D representation, we employ a pre-trained latent-Gaussian encoder-decoder architecture as shown in Fig. 2. A standard 3D Gaussian splatting scene is explicitly parameterized by a set of Gaussians \mathcal{G} . The Gaussian encoder E_{GS} compresses the high-dimensional Gaussians into the compact latent space: $\mathbf{z}_0 = E_{GS}(\mathcal{G})$. Then we apply noise to obtain \mathbf{z}_t . Conversely, after the conditioned diffusion process yields the denoised latent $\hat{\mathbf{z}}_0$, the decoder D_{GS} projects it back into the explicit 3D Gaussian space: $\hat{\mathcal{G}} = D_{GS}(\hat{\mathbf{z}}_0)$. This symmetric design ensures that our model can efficiently learn complex spatial distributions while ultimately generating high-fidelity 3D Gaussians.

3.4 Optimization

Our proposed Cog2Gen3D framework is supervised by training loss consists of three primary components: a latent diffusion loss \mathcal{L}_{diff} , an explicit node grounding loss \mathcal{L}_G , and a 3D Gaussian reconstruction loss \mathcal{L}_{recon} .

Latent Diffusion Loss \mathcal{L}_{diff} . To train the conditioned denoising network, we employ the standard latent diffusion objective, minimizing the mean squared error between the added noise ϵ and the predicted noise $\hat{\epsilon}$:

$$\mathcal{L}_{diff} = \mathbb{E}_{\mathbf{z}_0, \epsilon, t} [\|\epsilon - \hat{\epsilon}\|_2^2]. \quad (9)$$

Explicit Node Grounding Loss \mathcal{L}_g . Explicit scene graphs typically lack precise spatial grounding and contain sparse relations. Supervising latent edges with such limited data would bottleneck spatial reasoning. Therefore, we discard edge supervision and solely anchor the semantic identities of the nodes. Crucially, the dense nodes in our cognition graph do not strictly align with the sparse entities in the explicit graph. To address this, we dynamically select the top- K most critical latent nodes via cross-attention weight ranking that correspond to the K explicit entities. We pass these selected nodes through a classification head to output semantic probabilities p_i^{sem} . The loss is computed as a Cross-Entropy (CE) objective against the explicit semantic labels y_i^{sem} :

$$\mathcal{L}_g = \frac{1}{K} \sum_{i=1}^K \text{CE}(p_i^{sem}, y_i^{sem}). \quad (10)$$

This minimalist top- K supervision ensures semantic fidelity while granting the latent edges absolute freedom to autonomously infer complex 3D topology.

3D Gaussian Reconstruction Loss \mathcal{L}_{recon} . To guarantee metric precision and visual fidelity, we supervise the Gaussians $\hat{\mathcal{G}}$ using the ground-truth \mathcal{G} . This supervision is applied in the image space to ensure multi-view consistency. For a set of viewpoints v , we render the predicted Gaussians into images \hat{I}_v and compare them against the GT renders I_v , calculating L1 loss and D-SSIM loss:

$$\mathcal{L}_{recon} = \sum_v \left(\lambda_{L1} \|\hat{I}_v - I_v\|_1 + \lambda_{ssim} (1 - \text{SSIM}(\hat{I}_v, I_v)) \right). \quad (11)$$

Total Loss. The entire framework is optimized end-to-end using a weighted sum of the above three losses, which is formulated as:

$$\mathcal{L}_{total} = \lambda_1 \mathcal{L}_{diff} + \lambda_2 \mathcal{L}_g + \lambda_3 \mathcal{L}_{recon}, \quad (12)$$

where $\lambda_1, \lambda_2, \lambda_3$ are hyperparameters balancing the contributions of diffusion fidelity, structural cognition, and visual reconstruction.

4 Training Datasets and Pipeline

4.1 Our CogSG-3D Dataset

As shown in Fig. 6, to effectively train our Cog2Gen3D, we propose CogSG-3D, a comprehensive dataset aggregating pre-eminent public 3D datasets and self-built supplementary data from Marble World Labs [25]. It covers two categories:



Fig. 6: Statistics and examples of our proposed CogSG-3D dataset.

object-level (ShapeNet [26], Objaverse-XL [27], OmniObject3D [28], Pix3D [29], ABO [30], ModelNet [31]) and scene-level (ScanNet [32], 3D-Front [33]), ensuring diverse semantic and geometric distributions. To unify these heterogeneous source formats into a standardized format for training, our data processing pipeline encompasses three steps: 1) *Image prompt rendering*. We normalize the canonical poses of all 3D models and render 2D multi-view images to serve as visual prompts. 2) *Text prompt acquisition*. For datasets lacking explicit annotations, we leverage advanced Vision-Language Models (Gemini) to generate dense descriptive texts, ensuring rigorous vision-language alignment. 3) *Unified 3D Gaussians representation*. We convert all 3D ground truths into directly optimizable 3D Gaussians, overcoming the topological constraints of traditional meshes.

4.2 Training Pipeline

We design a progressive, three-stage training paradigm to ensure stable convergence and optimal semantic-geometric alignment:

Stage 1: Geometric-Latent Alignment. This stage aims to acquire latent representations of 3D scenes and a robust decoder. We pretrain a Gaussians auto-decoder where the encoder E_{GS} maps 3D Gaussians into a compact latent variable z and the decoder D_{GS} is simultaneously optimized to flawlessly reconstruct the 3D Gaussians from z , preserving rich semantic and geometric details.

Stage 2: Cognitive-Generative Alignment. The objective here is to synthesize semantically and geometrically coherent 3D latents guided by multimodal priors. Keeping the autoencoder frozen, we exclusively train the Latent Diffusion Model (LDM) in the z -space. The denoising network is conditioned on the 3D Latent Cognition Graph to enforce strict structural constraints.

Stage 3: End-to-End Fine-Tuning. This stage harmonizes the generative latent space with the explicit 3D rendering space. We unfreeze the decoder D_{GS} and jointly optimize it with the LDM end-to-end. This mitigates feature mismatch between synthesized latents and the decoder’s expected input distribution, significantly enhancing the overall visual fidelity and geometric precision.

Table 1: Text-to-3D comparison.					Table 2: Image-to-3D objects comparison.						
Method	T3Bench [34]				Method	ShapeNet [26]			OmniObject3D [28]		
	Single Obj.↑	Single w/ Surr.↑	Multi Obj.↑	Average↑		FID↓	KID(%)↓	MMD(%)↓	FID↓	KID(%)↓	MMD(%)↓
DreamFusion [3]	24.4	19.8	11.7	18.7	EG3D [35]	28.12	1.25	7.14	41.56	1.13	28.21
Magic3D [17]	37	35.4	25.7	32.7	GET3D [36]	38.62	1.85	6.45	49.41	1.53	13.57
SJC [4]	24.7	19.8	11.7	18.7	DHFRF [37]	98.53	6.14	8.59	147.59	8.82	16.07
Fantasia3D [15]	26.4	27	18.5	24	DiffTF [38]	26.58	1.15	6.15	25.36	0.81	6.64
ProlificDreamer [16]	49.4	44.8	35.8	43.3	DiffGS [39]	23.45	1.05	5.31	27.35	0.84	7.05
GaussianDreamer [18]	54	48.6	34.5	45.7	LN3Diff [40]	21.51	1.08	5.25	21.42	0.73	4.87
Ours	58.3	57.9	53.6	56.6	Ours	14.54	0.67	3.25	15.94	0.58	3.02



Fig. 7: Visualization of Text-to-3D on the T3-Bench dataset.

5 Experiments

5.1 Implementation Details

Our 3D latent cognition graph contains 64 hidden nodes by default, which can be manually adjusted according to scene complexity. For the diffusion process, we employ $T = 1000$ training timesteps, while a 50-step DDIM sampler is utilized for efficient inference. The total loss is optimized using the AdamW optimizer with a initial learning rate of 1×10^{-5} , where the loss weights in Eq. (12) are set as: $\lambda_1 = 0.8$, $\lambda_2 = 0.2$, and $\lambda_3 = 0.8$. All training and testing procedures are conducted on 8 NVIDIA A800 GPUs.

5.2 Comparison Experiments

Text-to-3D Generation. We evaluate text-to-3D generation on T3Bench [34] against SOTA methods [3, 4, 15–18]. We adopt the T3Bench quality scores across three complexity levels and their average. As shown in Tab. 1 and Fig. 6, the results demonstrate the superiority of our approach. Quantitatively, Cog2Gen3D achieves the highest scores across all metrics, with notable margins in the challenging multi-object task. Qualitatively, while baseline methods often suffer from blurred details, geometric distortions, or structural collapse in complex scenes due to the lack of spatial constraints, our method consistently produces high-fidelity 3D assets. Benefiting from the structural constraints of our 3D cognition graph, Cog2Gen3D maintains precise geometries and coherent multi-entity relationships, demonstrating significant advantages in holistic 3D scene generation.

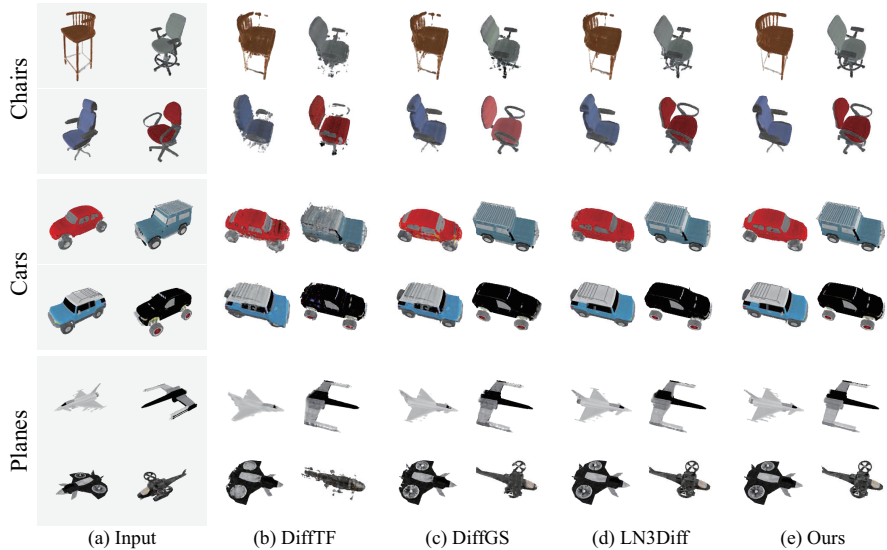


Fig. 8: Visualization of Image-to-3D objects on the ShapeNet dataset.

Image-to-3D Object Generation. We evaluate image-to-3D object generation on ShapeNet [26] and OmniObject3D [28] against leading baselines [35–40]. We adopt standard evaluation metrics such as FID, KID, and MMD. Tab. 2 and Fig. 8 shows that Cog2Gen3D establishes a clear advantage over existing baselines. Quantitatively, our model achieves the top scores across all metrics and datasets. Qualitatively, our framework reliably reconstructs detailed 3D assets. Leveraging the semantic and geometric perception of our 3D cognition graph, Cog2Gen3D excels at preserving high-fidelity appearances and plausible geometric structures.

Image-to-3D Scene Generation. We validate complex scene generation on 3D-Front [33] and our CogSG-3D datasets against semantic [41–45] and 2D geometry-guided [9, 14] baselines. We employ standard metrics such as Chamfer Distance (CD), F-Score, and IoU to evaluate the structural plausibility and visual fidelity of the generated 3D scenes. The quantitative results in Tab. 3 shows that Cog2Gen3D consistently outperforms all competing baselines. Visual comparisons in Fig. 9 reveal that existing approaches often struggle with scale inconsistencies, chaotic spatial layouts, or structural collapse when synthesizing cluttered spaces due to the lack of spatial awareness. Conversely, our model generates highly realistic and well-organized 3D environments by embedding semantic and absolute geometric cognitive features into the generation process.

5.3 Ablation Study

Effectiveness of Cognitive Feature Embeddings. A user study (Tab. 4) evaluates the distinct roles of the three cognitive tokens across Semantic Fidelity (SemF), Geometric Plausibility (GeoP), and Relational Coherence (RelC). Ablating the semantic, geometric, or logical tokens severely degrades SemF, GeoP, or RelC, respectively. This direct correspondence confirms that integrating all

Method	3D-Front [33]		
	Chamfer Dist.↓	F-Score↑	IoU↑
LucidDreamer [41]	0.083	50.79	0.536
SSR [42]	0.140	39.76	0.311
Gen3DSR [43]	0.123	40.07	0.363
REPARO [44]	0.129	41.68	0.339
MIDI [45]	0.080	50.19	0.518
EchoScene [9]	0.105	45.62	0.458
Layout2Scene [14]	0.094	48.36	0.492
Ours	0.063	58.43	0.682

Cognitive Tokens			User Study ↑		
Semantic	Geometric	Logical	SemF	GeoP	RelC
✓			4.12	2.38	2.15
	✓		2.23	4.08	2.74
		✓	2.41	2.58	3.92
✓	✓		4.38	4.35	2.82
✓		✓	4.42	2.75	4.28
	✓	✓	3.17	4.31	4.34
✓	✓	✓	4.65	4.58	4.62



Fig. 9: Visualization of Image-to-3D Scenes on 3D-Front and our CogSG-3D datasets.

three embeddings is essential for synthesizing scenes with high-fidelity semantics, plausible geometry, and coherent logic.

Superiority of Latent Graph Construction. We validate our structured topology by replacing it with a flattened token sequence (Tab. 5). This ablation degrades performance, indicating that flat sequences fail to capture complex 3D spatial dependencies. Conversely, our structured graph effectively models semantic-geometric interactions, significantly enhancing the structural rationality and geometric plausibility of generated scenes.

Impact of Dual-Stream Scene Graphs. We ablate the semantic and geometric streams to assess their contributions. Fig. 10 shows that removing either stream degrades performance. Moreover, omitting semantic graphs compromises texture fidelity and lacking geometric graphs causes severe structural distortions. This confirms both streams are indispensable for high-quality 3D generation.

5.4 Discussion

Correspondence between the Cognition Graph and 3D Scenes. To interpret the latent cognition graph, we compute attention maps between the generated 3D scenes and node/edge embeddings. Fig. 5 shows that high-attention regions precisely align with target objects and spatial boundaries. This confirms

Table 5: Graph cons. ablation.

Settings	3D-Front [33]		
	CD ↓	F-Score ↑	IoU ↑
w/o Graph	0.089	49.16	0.503
w/. Graph	0.063	58.43	0.683

Table 6: Geometry encoders.

Settings	3D-Front [33]		
	CD ↓	F-Score ↑	IoU ↑
ResNet50	0.091	48.75	0.498
CLIP ViT-L	0.076	53.88	0.591
VGGT	0.063	58.43	0.683

Table 7: Fusion strategy.

Settings	3D-Front [33]		
	CD ↓	F-Score ↑	IoU ↑
Concat.	0.085	50.41	0.523
Weighted	0.072	55.12	0.635
Common	0.063	58.43	0.683

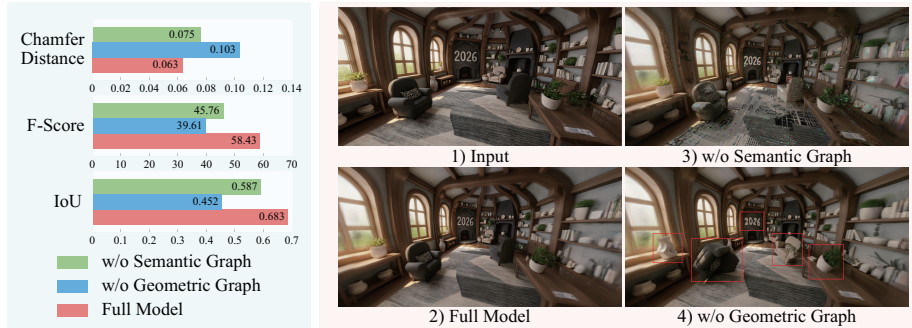


Fig. 10: Ablation of dual-stream scene graphs. Quantitative metrics drop noticeably without either stream. Qualitative examples reveal that omitting semantic or geometric graphs causes severe texture degradation or structural collapse, respectively.

that the graph acts as a structured cognitive map, successfully localizing semantic-geometric entities to bridge abstract prompts with 3D scenes.

Influence of the Geometry Perception Backbone. We evaluate different geometry encoders in Tab. 6. The VGGT encoder [19] achieves optimal performance by excelling at extracting robust geometric features and spatial structures. This provides precise absolute geometry guidance for the diffusion process, significantly enhancing the geometric plausibility of the generated 3D scenes.

Effectiveness of Common-based Fusion Strategy. We compare our common-based fusion against standard concatenation and weighted fusion. Tab. 7 shows that our approach effectively synergizes semantic and geometric features. This deep alignment preserves modality-specific priors, yielding the highest generation quality in both semantic fidelity and geometric plausibility.

Limitations. While Cog2Gen3D demonstrates strong capabilities in generating high-quality and geometrically plausible static 3D scenes, it currently struggles with dynamic 4D generation. This limitation primarily arises from the absence of temporal modeling within our framework. Our 3D cognition graph and Gaussian representation [24] are restricted to static constraints, failing to capture motion or topological evolution. Future work will integrate spatio-temporal graphs and 4D Gaussian Splatting [46] to enable the generation of spatially grounded and temporally consistent dynamic scenes.

6 Conclusion

In this work, we proposed Cog2Gen3D, a 3D cognition-guided diffusion framework designed to sculpture semantic-geometric cognition for high-quality 3D generation.

By integrating absolute geometric priors and semantic constraints, our method effectively resolves the challenges of scale inconsistency and the absence of spatial awareness prevalent in existing models. We introduced cognitive feature embeddings to map multi-modal information into a unified semantic-geometric space, and proposed the 3D latent cognition graph to capture complex spatial topological relationships and structural dependencies within 3D environments. Furthermore, we constructed the CogSG-3D dataset, providing extensive explicit scene graph and 3D Gaussian annotations to support training. The superiority of our approach has been demonstrated through extensive experiments across multiple tasks, including text-to-3D, image-to-3D object, and complex scene generation, affirming its effectiveness in modeling the physical world.

References

1. Lvmin Zhang, Anyi Rao, and Maneesh Agrawala. Adding conditional control to text-to-image diffusion models. In *Proceedings of the IEEE/CVF international conference on computer vision*, pages 3836–3847, 2023. [1](#)
2. Andreas Blattmann, Tim Dockhorn, Sumith Kulal, Daniel Mendeleevitch, Maciej Kilian, Dominik Lorenz, Yam Levi, Zion English, Vikram Voleti, Adam Letts, et al. Stable video diffusion: Scaling latent video diffusion models to large datasets. *arXiv preprint arXiv:2311.15127*, 2023. [1](#)
3. Ben Poole, Ajay Jain, Jonathan T Barron, and Ben Mildenhall. Dreamfusion: Text-to-3d using 2d diffusion. *arXiv preprint arXiv:2209.14988*, 2022. [1](#), [4](#), [11](#)
4. Haochen Wang, Xiaodan Du, Jiahao Li, Raymond A Yeh, and Greg Shakhnarovich. Score jacobian chaining: Lifting pretrained 2d diffusion models for 3d generation. In *Proceedings of the IEEE/CVF conference on computer vision and pattern recognition*, pages 12619–12629, 2023. [1](#), [4](#), [11](#)
5. Kai Wang, Yu-An Lin, Ben Weissmann, Manolis Savva, Angel X Chang, and Daniel Ritchie. Planit: Planning and instantiating indoor scenes with relation graph and spatial prior networks. *ACM Transactions on Graphics (TOG)*, 38(4):1–15, 2019. [2](#), [4](#)
6. Helisa Dhamo, Fabian Manhardt, Nassir Navab, and Federico Tombari. Graph-to-3d: End-to-end generation and manipulation of 3d scenes using scene graphs. In *Proceedings of the IEEE/CVF International Conference on Computer Vision*, pages 16352–16361, 2021. [2](#), [4](#)
7. Guangyao Zhai, Evin Pinar Örnek, Shun-Cheng Wu, Yan Di, Federico Tombari, Nassir Navab, and Benjamin Busam. Commonsences: Generating commonsense 3d indoor scenes with scene graph diffusion. *Advances in Neural Information Processing Systems*, 36:30026–30038, 2023. [2](#), [4](#)
8. Chenguo Lin and Yadong Mu. Instructscene: Instruction-driven 3d indoor scene synthesis with semantic graph prior. *arXiv preprint arXiv:2402.04717*, 2024. [2](#), [4](#)
9. Guangyao Zhai, Evin Pinar Örnek, Dave Zhenyu Chen, Ruotong Liao, Yan Di, Nassir Navab, Federico Tombari, and Benjamin Busam. Echoscene: Indoor scene generation via information echo over scene graph diffusion. In *European Conference on Computer Vision*, pages 167–184. Springer, 2024. [2](#), [4](#), [12](#), [13](#)
10. Manyi Li, Akshay Gadi Patil, Kai Xu, Siddhartha Chaudhuri, Owais Khan, Ariel Shamir, Changhe Tu, Baoquan Chen, Daniel Cohen-Or, and Hao Zhang. Grains: Generative recursive autoencoders for indoor scenes. *ACM Transactions on Graphics (TOG)*, 38(2):1–16, 2019. [2](#), [4](#)

11. Sherwin Bahmani, Jeong Joon Park, Despoina Paschalidou, Xingguang Yan, Gordon Wetzstein, Leonidas Guibas, and Andrea Tagliasacchi. Cc3d: Layout-conditioned generation of compositional 3d scenes. In *Proceedings of the IEEE/CVF International Conference on Computer Vision*, pages 7171–7181, 2023. 2, 4
12. Ryan Po and Gordon Wetzstein. Compositional 3d scene generation using locally conditioned diffusion. In *2024 International Conference on 3D Vision (3DV)*, pages 651–663. IEEE, 2024. 2, 4
13. Xiuyu Yang, Yunze Man, Junkun Chen, and Yu-Xiong Wang. Scenecraft: Layout-guided 3d scene generation. *Advances in Neural Information Processing Systems*, 37:82060–82084, 2024. 2, 4
14. Minglin Chen, Longguang Wang, Sheng Ao, Ye Zhang, Kai Xu, and Yulan Guo. Layout2scene: 3d semantic layout guided scene generation via geometry and appearance diffusion priors. *arXiv preprint arXiv:2501.02519*, 2025. 2, 4, 12, 13
15. Rui Chen, Yongwei Chen, Ningxin Jiao, and Kui Jia. Fantasia3d: Disentangling geometry and appearance for high-quality text-to-3d content creation. In *Proceedings of the IEEE/CVF international conference on computer vision*, pages 22246–22256, 2023. 4, 11
16. Zhengyi Wang, Cheng Lu, Yikai Wang, Fan Bao, Chongxuan Li, Hang Su, and Jun Zhu. Prolificdreamer: High-fidelity and diverse text-to-3d generation with variational score distillation. *Advances in neural information processing systems*, 36:8406–8441, 2023. 4, 11
17. Chen-Hsuan Lin, Jun Gao, Luming Tang, Towaki Takikawa, Xiaohui Zeng, Xun Huang, Karsten Kreis, Sanja Fidler, Ming-Yu Liu, and Tsung-Yi Lin. Magic3d: High-resolution text-to-3d content creation. In *Proceedings of the IEEE/CVF conference on computer vision and pattern recognition*, pages 300–309, 2023. 4, 11
18. Taoran Yi, Jiemin Fang, Junjie Wang, Guanjun Wu, Lingxi Xie, Xiaopeng Zhang, Wenyu Liu, Qi Tian, and Xinggang Wang. Gaussiandreamer: Fast generation from text to 3d gaussians by bridging 2d and 3d diffusion models. In *Proceedings of the IEEE/CVF conference on computer vision and pattern recognition*, pages 6796–6807, 2024. 4, 11
19. Jianyuan Wang, Minghao Chen, Nikita Karaev, Andrea Vedaldi, Christian Rupprecht, and David Novotny. Vggt: Visual geometry grounded transformer. In *Proceedings of the Computer Vision and Pattern Recognition Conference*, pages 5294–5306, 2025. 4, 5, 14
20. Yining Hong, Haoyu Zhen, Peihao Chen, Shuhong Zheng, Yilun Du, Zhenfang Chen, and Chuang Gan. 3d-llm: Injecting the 3d world into large language models. *Advances in Neural Information Processing Systems*, 36:20482–20494, 2023. 4
21. Runsen Xu, Xiaolong Wang, Tai Wang, Yilun Chen, Jiangmiao Pang, and Dahua Lin. Pointllm: Empowering large language models to understand point clouds. In *European Conference on Computer Vision*, pages 131–147. Springer, 2024. 4
22. Kaiming He, Xiangyu Zhang, Shaoqing Ren, and Jian Sun. Deep residual learning for image recognition. In *Proceedings of the IEEE conference on computer vision and pattern recognition*, pages 770–778, 2016. 5
23. Alec Radford, Jong Wook Kim, Chris Hallacy, Aditya Ramesh, Gabriel Goh, Sandhini Agarwal, Girish Sastry, Amanda Askell, Pamela Mishkin, Jack Clark, et al. Learning transferable visual models from natural language supervision. In *International conference on machine learning*, pages 8748–8763. PmLR, 2021. 6
24. Bernhard Kerbl, Georgios Kopanas, Thomas Leimkühler, George Drettakis, et al. 3d gaussian splatting for real-time radiance field rendering. *ACM Trans. Graph.*, 42(4):139–1, 2023. 14

25. World Labs. Marble: A multimodal world model. <https://www.worldlabs.ai/blog/marble-world-model>, November 2025. Accessed: 2026-03-02. 9
26. Angel X Chang, Thomas Funkhouser, Leonidas Guibas, Pat Hanrahan, Qixing Huang, Zimo Li, Silvio Savarese, Manolis Savva, Shuran Song, Hao Su, et al. Shapenet: An information-rich 3d model repository. *arXiv preprint arXiv:1512.03012*, 2015. 10, 11, 12
27. Matt Deitke, Ruoshi Liu, Matthew Wallingford, Huong Ngo, Oscar Michel, Aditya Kusupati, Alan Fan, Christian Laforte, Vikram Voleti, Samir Yitzhak Gadre, et al. Objaverse-xl: A universe of 10m+ 3d objects. *Advances in Neural Information Processing Systems*, 36:35799–35813, 2023. 10
28. Tong Wu, Jiarui Zhang, Xiao Fu, Yuxin Wang, Jiawei Ren, Liang Pan, Wayne Wu, Lei Yang, Jiaqi Wang, Chen Qian, et al. Omniobject3d: Large-vocabulary 3d object dataset for realistic perception, reconstruction and generation. In *Proceedings of the IEEE/CVF conference on computer vision and pattern recognition*, pages 803–814, 2023. 10, 11, 12
29. Xingyuan Sun, Jiajun Wu, Xiuming Zhang, Zhoutong Zhang, Chengkai Zhang, Tianfan Xue, Joshua B Tenenbaum, and William T Freeman. Pix3d: Dataset and methods for single-image 3d shape modeling. In *Proceedings of the IEEE conference on computer vision and pattern recognition*, pages 2974–2983, 2018. 10
30. Jasmine Collins, Shubham Goel, Kenan Deng, Achleshwar Luthra, Leon Xu, Erhan Gundogdu, Xi Zhang, Tomas F Yago Vicente, Thomas Dideriksen, Himanshu Arora, et al. Abo: Dataset and benchmarks for real-world 3d object understanding. In *Proceedings of the IEEE/CVF conference on computer vision and pattern recognition*, pages 21126–21136, 2022. 10
31. Zhirong Wu, Shuran Song, Aditya Khosla, Fisher Yu, Linguang Zhang, Xiaoou Tang, and Jianxiong Xiao. 3d shapenets: A deep representation for volumetric shapes. In *Proceedings of the IEEE conference on computer vision and pattern recognition*, pages 1912–1920, 2015. 10
32. Angela Dai, Angel X Chang, Manolis Savva, Maciej Halber, Thomas Funkhouser, and Matthias Nießner. Scannet: Richly-annotated 3d reconstructions of indoor scenes. In *Proceedings of the IEEE conference on computer vision and pattern recognition*, pages 5828–5839, 2017. 10
33. Huan Fu, Bowen Cai, Lin Gao, Ling-Xiao Zhang, Jiaming Wang, Cao Li, Qixun Zeng, Chengyue Sun, Rongfei Jia, Binqiang Zhao, et al. 3d-front: 3d furnished rooms with layouts and semantics. In *Proceedings of the IEEE/CVF International Conference on Computer Vision*, pages 10933–10942, 2021. 10, 12, 13, 14
34. Yuze He, Yushi Bai, Matthieu Lin, Wang Zhao, Yubin Hu, Jenny Sheng, Ran Yi, Juanzi Li, and Yong-Jin Liu. T3bench: Benchmarking current progress in text-to-3d generation. *arXiv preprint arXiv:2310.02977*, 2023. 11
35. Eric R Chan, Connor Z Lin, Matthew A Chan, Koki Nagano, Boxiao Pan, Shalini De Mello, Orazio Gallo, Leonidas J Guibas, Jonathan Tremblay, Sameh Khamis, et al. Efficient geometry-aware 3d generative adversarial networks. In *Proceedings of the IEEE/CVF conference on computer vision and pattern recognition*, pages 16123–16133, 2022. 11, 12
36. Jun Gao, Tianchang Shen, Zian Wang, Wenzheng Chen, Kangxue Yin, Daiqing Li, Or Litany, Zan Gojcic, and Sanja Fidler. Get3d: A generative model of high quality 3d textured shapes learned from images. *Advances in neural information processing systems*, 35:31841–31854, 2022. 11, 12
37. Norman Müller, Yawar Siddiqui, Lorenzo Porzi, Samuel Rota Bulo, Peter Kotschieder, and Matthias Nießner. Diffrf: Rendering-guided 3d radiance field

- diffusion. In *Proceedings of the IEEE/CVF conference on computer vision and pattern recognition*, pages 4328–4338, 2023. [11](#), [12](#)
38. Ziang Cao, Fangzhou Hong, Tong Wu, Liang Pan, and Ziwei Liu. Large-vocabulary 3d diffusion model with transformer. *arXiv preprint arXiv:2309.07920*, 2023. [11](#), [12](#)
 39. Junsheng Zhou, Weiqi Zhang, and Yu-Shen Liu. Diffgs: Functional gaussian splatting diffusion. *Advances in Neural Information Processing Systems*, 37:37535–37560, 2024. [11](#), [12](#)
 40. Yushi Lan, Fangzhou Hong, Shuai Yang, Shangchen Zhou, Xuyi Meng, Bo Dai, Xingang Pan, and Chen Change Loy. Ln3diff: Scalable latent neural fields diffusion for speedy 3d generation. In *ECCV*, 2024. [11](#), [12](#)
 41. Jaeyoung Chung, Suyoung Lee, Hyeongjin Nam, Jaerin Lee, and Kyoung Mu Lee. Luciddreamer: Domain-free generation of 3d gaussian splatting scenes. *arXiv preprint arXiv:2311.13384*, 2023. [12](#), [13](#)
 42. Yixin Chen, Junfeng Ni, Nan Jiang, Yaowei Zhang, Yixin Zhu, and Siyuan Huang. Single-view 3d scene reconstruction with high-fidelity shape and texture. In *2024 International Conference on 3D Vision (3DV)*, pages 1456–1467. IEEE, 2024. [12](#), [13](#)
 43. Andreea Ardelean, Mert Özer, and Bernhard Egger. Gen3dsr: Generalizable 3d scene reconstruction via divide and conquer from a single view. In *2025 International Conference on 3D Vision (3DV)*, pages 616–626. IEEE, 2025. [12](#), [13](#)
 44. Haonan Han, Rui Yang, Huan Liao, Jiankai Xing, Zunnan Xu, Xiaoming Yu, Junwei Zha, Xiu Li, and Wanhua Li. Reparo: Compositional 3d assets generation with differentiable 3d layout alignment. In *Proceedings of the IEEE/CVF International Conference on Computer Vision*, pages 25367–25377, 2025. [12](#), [13](#)
 45. Zehuan Huang, Yuan-Chen Guo, Xingqiao An, Yunhan Yang, Yangguang Li, Zi-Xin Zou, Ding Liang, Xihui Liu, Yan-Pei Cao, and Lu Sheng. Midi: Multi-instance diffusion for single image to 3d scene generation. In *Proceedings of the IEEE/CVF Conference on Computer Vision and Pattern Recognition*, pages 23646–23657, 2025. [12](#), [13](#)
 46. Guanjun Wu, Taoran Yi, Jiemin Fang, Lingxi Xie, Xiaopeng Zhang, Wei Wei, Wenyu Liu, Qi Tian, and Xingang Wang. 4d gaussian splatting for real-time dynamic scene rendering. In *Proceedings of the IEEE/CVF conference on computer vision and pattern recognition*, pages 20310–20320, 2024. [14](#)